

# Quantum-limited directional amplifiers with optomechanics

Daniel Malz,<sup>1</sup> László D. Tóth,<sup>2</sup> Nathan R. Bernier,<sup>2</sup> Alexey K. Feofanov,<sup>2</sup> Tobias J. Kippenberg,<sup>2</sup> and Andreas Nunnenkamp<sup>1</sup>

<sup>1</sup>*Cavendish Laboratory, University of Cambridge, Cambridge CB3 0HE, United Kingdom*

<sup>2</sup>*Institute of Physics, École Polytechnique Fédérale de Lausanne, Lausanne 1015, Switzerland*

(Dated: January 27, 2023)

Directional amplifiers are an important resource in quantum information processing, as they protect sensitive quantum systems from excess noise. Here, we propose an implementation of phase-preserving and phase-sensitive directional amplifiers for microwave signals in an electromechanical setup comprising two microwave cavities and two mechanical resonators. We show that both can reach their respective quantum limits on added noise. In the reverse direction, they emit thermal noise stemming from the mechanical resonators and we discuss how this noise can be suppressed, a crucial aspect for technological applications. The isolation bandwidth in both is of the order of the mechanical linewidth divided by the amplitude gain. We derive the bandwidth and gain-bandwidth product for both and find that the phase-sensitive amplifier has an unlimited gain-bandwidth product. Our study represents an important step toward flexible, on-chip integrated nonreciprocal amplifiers of microwave signals.

**Introduction.**—Nonreciprocal transmission and amplification of signals are essential to communication and signal processing, as they protect the signal source from extraneous noise. Conventional ferrite-based devices rely on magnetic fields and are challenging to integrate in superconducting circuits. Hence, there exists strong incentive to find more suitable implementations [1–12]. In the microwave domain, the strong Josephson nonlinearity and parametric pumping can achieve both photon gain and conversion processes, which have been exploited to realize circulators and directional amplifiers in a superconducting circuit architecture [5, 11–13]. Another promising platform is optomechanics, where nonreciprocal devices [4, 5, 14–22], phase-preserving amplifiers [25–28], and phase-sensitive amplifiers [29–32] have been proposed and realized.

In recent theoretical work Ranzani and Aumentado [14, 15] have analyzed the general conditions for nonreciprocity in parametrically coupled systems, and shown that nonreciprocity arises due to dissipation in ancillary modes and multi-path interference. Metelmann and Clerk [16] have shown that any coherent interaction can be made directional by balancing it with a dissipative process. Indeed, this insight led to a demonstration of nonreciprocity using optomechanics in the optical domain [17], and theoretical investigations into minimal implementations of directional amplifiers [18].

While implementing the balance between a *direct* coherent coupling between the cavities and a dissipative interaction is challenging experimentally, Refs. [4, 5] have recently demonstrated nonreciprocal transmission between two cavity modes where two mechanical resonators each mediate both coherent and dissipative coupling. Here, building on this concept, we propose directional amplifiers using exclusively optomechanical interactions. Microwave tones on the red and blue sidebands enable so-called beam-splitter and two-mode squeezing interactions (cf. Fig. 1), leading to a total of eight controllable terms in the Hamiltonian. We identify and analyze a simple directional phase-preserving amplifier that uses four drives and a directional phase-sensitive amplifier using six drives. While the gain-bandwidth product of the phase-preserving amplifier is limited to the cavity decay rate, the phase-sensitive amplifier has an unlimited gain-bandwidth product. We show that both

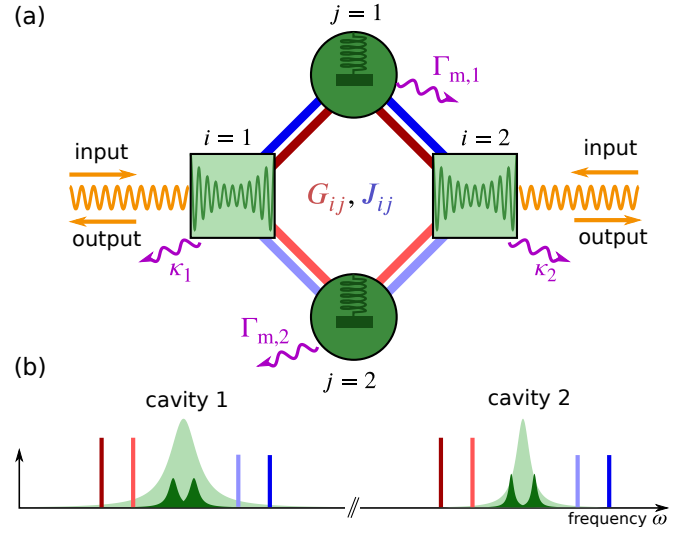


FIG. 1. (Color online.) (a) Schematic of all possible interactions in optomechanical plaquette comprising two mechanical resonators (round, dark green) and two cavities (square, light green). The cavities [light green Lorentzians in (b)] are driven by up to eight tones, placed close to the mechanical sidebands, at frequencies  $\omega_{c,i} \pm (\Omega_j + \delta_j)$ , as illustrated in (b), which induce hopping and two-mode squeezing interactions ( $G_{ij}, J_{ij}$ ), denoted in (a) by red and blue lines connecting the modes. This leads to the time-independent Hamiltonian (1).

amplifiers can reach their quantum limits of a half and zero added quanta, respectively, and emit thermal noise from the mechanical resonators in the reverse direction, a necessary consequence of impedance matching and directionality. We show how the reverse noise can be reduced through additional sideband cooling without interfering with directionality or amplification. Our concrete proposal bridges the gap between previous theoretical studies and experimental realization and therefore represents an important step toward on-chip integrated nonreciprocal amplifiers of microwave signals.

**Model.**—We consider an optomechanical plaquette, comprising two microwave cavities coupled via two mechanical resonators, as shown in Fig. 1(a). The cavities are driven close

to the motional sidebands. After a standard treatment, which includes linearizing the Hamiltonian, neglecting counterrotating terms, and going into a rotating frame [2, 33], we arrive at the time-independent Hamiltonian ( $\hbar = 1$ )

$$H_{\text{sys}} = - \sum_{i,j} \delta_i b_j^\dagger b_j - \sum_{i,j=1}^2 \left[ a_i^\dagger (G_{ij} b_j + J_{ij} b_j^\dagger) + \text{H.c.} \right], \quad (1)$$

where  $a_i$  ( $b_i$ ) is the annihilation operator for the  $i$ th cavity mode (mechanical resonator),  $G_{ij} = \alpha_{ij} - g_{0,ij}$  and  $J_{ij} = \alpha_{ij} + g_{0,ij}$  are field-enhanced optomechanical coupling strengths,  $\alpha_{ij\pm}$  is the amplitude of the coherent state produced in cavity  $i$  due to a pump at frequency  $\omega_{c,i} \pm (\Omega_j + \delta_j)$ , and  $g_{0,ij}$  are the vacuum optomechanical couplings. Since the couplings  $G_{ij}$ ,  $J_{ij}$  depend on the pumps, their amplitude and phase can be controlled. The interactions are represented in Figs. 1(a), 2(a), 3(a) as red ( $G_{ij}$ ) and blue ( $J_{ij}$ ) lines. Further details can be found in the Supplementary Information (SI), including the justification for neglecting the off-resonant terms.

We describe the system with quantum Langevin equations [1–3]. Neglecting mechanical noise (analyzed later), and eliminating the mechanical modes, we obtain

$$\sum_{j=1}^2 [\chi_{c,i}^{-1}(\omega) \delta_{ij} + i\mathbf{T}_{ij}(\omega)] \vec{A}_j(\omega) = \sqrt{\kappa_i} \vec{A}_{i,\text{in}}(\omega), \quad (2)$$

where the susceptibility  $\chi_{c,i}(\omega) = [\kappa_i/2 - i\omega]^{-1}$ . Each  $i\mathbf{T}_{ij}$  is a 2-by-2 matrix that acts on the vector  $\vec{A}_j = (a_j, a_j^\dagger)^T$ , and is

$$i\mathbf{T}_{ij}(\omega) = \sum_{k=1}^2 \sigma_z \left[ \chi_{m,k}(\omega) \begin{pmatrix} G_{ik} G_{jk}^* & G_{ik} J_{jk} \\ J_{ik}^* G_{jk}^* & J_{ik}^* J_{jk} \end{pmatrix} - \chi_{m,k}^*(-\omega) \begin{pmatrix} J_{ik} J_{jk}^* & J_{ik} G_{jk} \\ G_{ik}^* J_{jk}^* & G_{ik}^* G_{jk} \end{pmatrix} \right], \quad (3)$$

where  $\sigma_z = \text{diag}(1, -1)$  and  $\chi_{m,i}(\omega) = [\Gamma_{m,i}/2 - i(\omega + \delta_i)]^{-1}$ .  $i\mathbf{T}_{ii}$  is akin to a self-energy for mode  $A_i$ , whereas  $i\mathbf{T}_{ij}$  for  $i \neq j$  is a matrix of coupling strengths between the modes. Since the interaction is mediated by mechanical resonators, their susceptibility  $\chi_{m,i}$  appears in the coupling matrix.

Using the input-output relation  $a_{i,\text{out}} = a_{i,\text{in}} - \sqrt{\kappa_i} a_i$ , [3] the optical scattering matrix is  $\mathbf{S}_{\text{optical}}(\omega) = \mathbb{I}_4 - \mathbf{L}\chi(\omega)\mathbf{L}$ , where  $\mathbf{L} = \text{diag}(\sqrt{\kappa_1}, \sqrt{\kappa_1}, \sqrt{\kappa_2}, \sqrt{\kappa_2})$ , and

$$[\chi(\omega)]^{-1} = \begin{pmatrix} \chi_{c,1}^{-1}(\omega) \mathbb{I}_2 + i\mathbf{T}_{11}(\omega) & i\mathbf{T}_{12}(\omega) \\ i\mathbf{T}_{21}(\omega) & \chi_{c,2}^{-1}(\omega) \mathbb{I}_2 + i\mathbf{T}_{22}(\omega) \end{pmatrix}. \quad (4)$$

We say the system is nonreciprocal if the moduli of forward and reverse scattering amplitudes differ, which occurs if  $|\mathbf{T}_{12}| \neq |\mathbf{T}_{21}|$ . Looking for instance at the top left elements  $[i\mathbf{T}_{12}]_{11}$ ,  $[i\mathbf{T}_{21}]_{11}$ , we see that nonreciprocity can arise because flipping directionality ( $1 \leftrightarrow 2$ ) conjugates the complex couplings, but leaves the mechanical susceptibility unchanged. Nonreciprocity can also be understood in the framework presented in Ref. [16], as we outline in the SI.

*Directional phase-preserving amplifier (DPPA).*—We consider the coupling amplitudes [cf. Fig. 2(a)]

$$\mathbf{G} = \frac{1}{2} \begin{pmatrix} e^{i\Phi/2} \sqrt{C_1 \Gamma_{m,1} \kappa_1} & e^{-i\Phi/2} \sqrt{C_1 \Gamma_{m,2} \kappa_1} \\ 0 & 0 \end{pmatrix}, \quad (5)$$

$$\mathbf{J} = \frac{1}{2} \begin{pmatrix} 0 & 0 \\ \sqrt{C_2 \Gamma_{m,1} \kappa_2} & \sqrt{C_2 \Gamma_{m,2} \kappa_2} \end{pmatrix},$$

that is, the first (second) cavity has two drives, close to the lower (upper) motional sidebands corresponding to the mechanical resonators [cf. Fig. 2(a-b)]. We have already written the amplitudes in terms of cooperativities  $C_{1i} = 4|G_{1i}|^2/(\kappa_1 \Gamma_{m,i})$ ,  $C_{2i} = 4|J_{2i}|^2/(\kappa_2 \Gamma_{m,i})$ , and chosen the cooperativities in both arms to be equal  $C_1 \equiv C_{1i}$ ,  $C_2 \equiv C_{2i}$ . Given Eqs. (2) and (5), isolation ( $\mathbf{T}_{12} = 0$ ) requires  $\delta_1^2 \Gamma_{m,2}^2 = \delta_2^2 \Gamma_{m,1}^2$  [37].  $\delta_1$  and  $\delta_2$  must have opposite signs, since otherwise the phase  $[\arg(\chi_{m,j})]$  in both arms is the same, which could cause forward and reverse transmission to vanish simultaneously (“double isolation”) (cf. SI). Thus, we parametrize both detunings by a single dimensionless variable  $\delta_1 = \delta \Gamma_{m,1}$ ,  $\delta_2 = -\delta \Gamma_{m,2}$ .

Isolation occurs for certain values of the coupling amplitudes  $\theta_{1i} \equiv \arg(G_{1i})$  and  $\theta_{2i} \equiv \arg(J_{2i})$ . First note that a change  $b_i \rightarrow b_i e^{i\psi}$ , equivalent to an inconsequential translation in time, causes an opposite change in phase of  $G_{1i}$  and  $J_{2i}$  [see Eq. (1)]. Similarly, the phase at the cavities is immaterial. Thus, the only relevant phase is the overall relative phase, the “plaquette phase”,  $\Phi \equiv \theta_{11} + \theta_{21} - \theta_{12} - \theta_{22}$ , which explains the parametrization in Eq. (5). Choosing the detuning parameter  $\delta = \sqrt{2C_1 - 1}/2$  to achieve impedance matching (i.e., vanishing reflection at cavity 1), which is possible for  $C_1 \geq 0.5$ , the plaquette phase at which isolation occurs is

$$\Phi = i \log \left( \frac{2\delta - i}{2\delta + i} \right) = 2 \arccos \sqrt{1 - 1/(2C_1)}. \quad (6)$$

It is related to the mechanical susceptibilities via  $\arg[\chi_{m,1}(0)] = (\pi - \Phi)/2 = \arg[\chi_{m,2}^*(0)]$ . Inverting the plaquette phase  $-\Phi$  leads to isolation in the opposite direction (cf. SI).

We have chosen the couplings in Eq. (5) due to the following reasons. First, we need an even number of blue and red tones to obtain equivalent arms of the circuit. Second, without blue drives amplification cannot occur, as the resulting Hamiltonian is number conserving. Third, a directional amplifier with four blue drives is possible, but it cannot be impedance matched to the signal source (cf. SI). Last, swapping hopping and amplifier interactions in one arm of the circuit cannot lead to directional amplification [38].

The condition  $C_2 < C_1$  ensures that the system does not exceed the parametric instability threshold. In the limit of large gain, we obtain our first main result, the scattering matrix

$$\begin{pmatrix} a_{1,\text{out}}(0) \\ a_{2,\text{out}}^\dagger(0) \end{pmatrix} = \begin{pmatrix} \frac{1}{\sqrt{2}} & -\frac{1}{\sqrt{2}} & 0 & 0 \\ \frac{i\sqrt{G}}{\sqrt{4C_1}} & \frac{i\sqrt{G}}{\sqrt{4C_1}} & -\sqrt{G} & \frac{C_1+C_2}{C_2-C_1} \end{pmatrix} \begin{pmatrix} b_{1,\text{in}}(0) \\ b_{2,\text{in}}(0) \\ a_{1,\text{in}}(0) \\ a_{2,\text{in}}^\dagger(0) \end{pmatrix}, \quad (7)$$

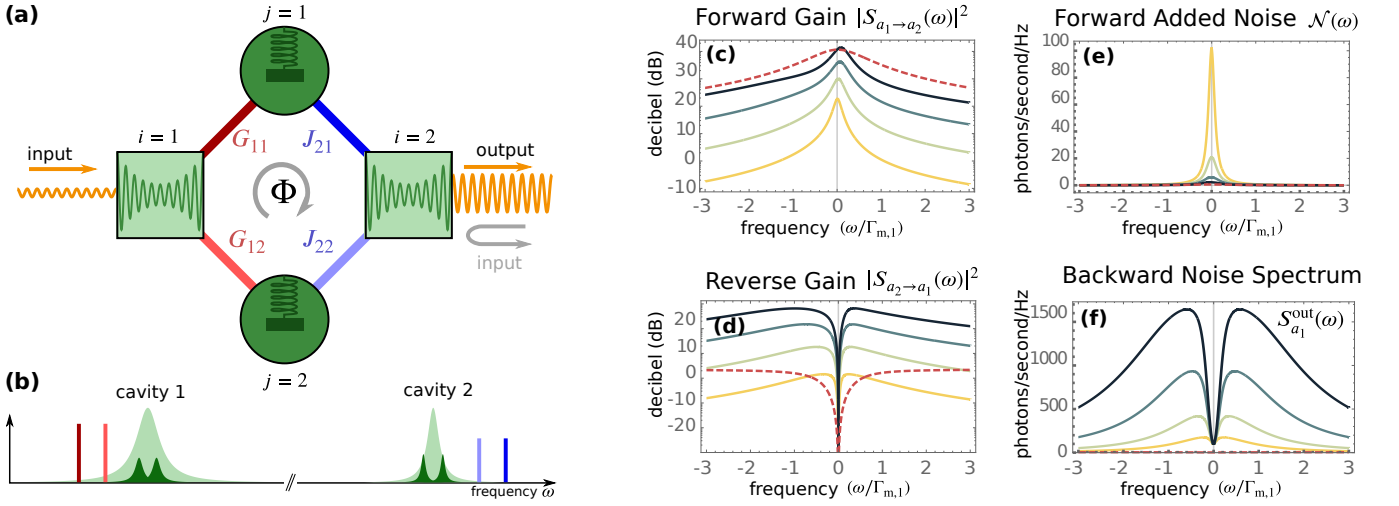


FIG. 2. (Color online.) The directional phase-preserving amplifier (DPPA). (a) Model. Red hopping interactions are impedance matched, blue provide the amplification. (b) Pump setup. Cavity 1 (cavity 2) is pumped on the red (blue) sidebands of the mechanical resonators. In (c-f) we plot forward gain, reverse gain [cf. Eq. (7)], added noise [Eq. (9)], and the output noise fluctuation spectrum of cavity 1, all as functions of frequency in units of  $\Gamma_{m,1}$ , for cooperativities  $C_1 = \{1, 3, 10, 30\}$ ,  $C_2 = C_1 - 0.1\sqrt{C_1}$  (yellow to black, or light to dark). Parameters are  $\kappa_2/\kappa_1 = 0.7$ ,  $\Gamma_{m,1}/\kappa_1 = 10^{-2}$ ,  $\Gamma_{m,2}/\Gamma_{m,1} = 0.8$ , thermal occupation of the mechanical resonators  $n_{m,1} = n_{m,2} = 100$ , and cavities  $n_{c,1} = n_{c,2} = 0$ . External sideband cooling with an auxiliary mode can achieve  $n_{m,j} \approx 0$ , without negatively affecting amplification properties, as discussed below. The red (dashed) curve in each plot illustrates this case, with  $C_1 = 30$  and effective parameters  $n_{\text{eff},i} = n_{m,i}(\Gamma_{m,i}/\Gamma_{\text{eff},i})$ ,  $\Gamma_{\text{eff},i} = 50\Gamma_{m,i}$ .

with vanishing reverse gain  $S_{a_2 \rightarrow a_1}(0)$ , but forward gain

$$|S_{a_1 \rightarrow a_2}(0)|^2 \equiv \mathcal{G} = \frac{4C_1C_2}{(C_1 - C_2)^2}, \quad (8)$$

which can in principle be arbitrarily large.

At the same time, thermal noise from the mechanical resonators is suppressed by increasing  $C_1$ , as is demonstrated in Fig. 2(e), where we plot the noise added to the signal  $\mathcal{N}(\omega) = \mathcal{G}^{-1} \sum_{i \neq a_1} (n_i + 1/2) |S_{i \rightarrow a_2}(\omega)|^2$  [27, 33, 39], where we sum over all noise sources, with associated thermal occupation  $n_i$ , and scattering amplitude to the second cavity  $S_{i \rightarrow a_2}$ . Using Eq. (7), assuming thermal occupations  $n_{c,i}$  ( $n_{m,i}$ ) for the  $i$ th cavity mode (mechanical resonator), on resonance it evaluates to

$$\mathcal{N}_{\text{DPPA}} = \frac{1}{4C_1} (n_{m,1} + n_{m,2} + 1) + \frac{(C_1 + C_2)^2}{4C_1C_2} \left( n_{c,2} + \frac{1}{2} \right). \quad (9)$$

As a result, for large  $C_1 \gtrsim C_2$ , and vanishing thermal occupation of the cavity input, we reach the quantum limit of half a quantum of added noise,  $\mathcal{N}_{\text{DPPA}} \rightarrow 1/2$  [33, 39].

Another important figure of merit is noise emerging from cavity 1, characterized by the output noise spectral density,  $S_{a_1}^{\text{out}}(\omega) \equiv \frac{1}{2} \int \frac{d\omega'}{2\pi} \langle a_{1,\text{out}}^\dagger(\omega) a_{1,\text{out}}(\omega') + a_{1,\text{out}}(\omega) a_{1,\text{out}}^\dagger(\omega') \rangle$ , which we plot in Fig. 2(f). Ultimately, the reason for building directional amplifiers is to reduce this figure. On resonance,  $S_{1,\text{out}}^{\text{DPPA}}(0) = (n_{m,1} + n_{m,2} + 1)/2$ . The same discussion applies to both amplifiers presented here, and can be found below.

The off-resonance behavior of the DPPA is remarkably rich and depends on the dimensionless quantities  $\kappa_i/\Gamma_{m,j}$ ,  $C_1$ ,  $C_2$ . We plot forward gain, reverse gain, added noise, and the noise

spectrum at cavity 1 as functions of frequency at cooperativities  $C_1 = \{1, 3, 10, 30\}$ ,  $C_2 = C_1 - 0.1\sqrt{C_1}$  in Fig. 2(c-f).  $C_2$  is chosen such that when increasing  $C_1$  both gain and bandwidth are enhanced.

We show in the SI that for  $\Gamma_{m,j} = \Gamma_m$  and  $\kappa_i = \kappa$  and in the regime where  $\kappa/\Gamma_m \gg \{1, C_1, C_2\}$  the gain bandwidth is  $\Gamma = 4\sqrt{C_1C_2}\Gamma_m$  [cf. Fig. 2(c)]. As the gain gets large and  $C_1, C_2$  dominate the other dimensionless parameters, the bandwidth approaches  $\Gamma = \kappa(C_1 - C_2)/C_1$ , leading to the gain-bandwidth product limit  $P \equiv \Gamma\sqrt{\mathcal{G}} \rightarrow 2\kappa$ , independent of the ratio  $\kappa/\Gamma_m$ . Close to resonance, the reverse scattering amplitude  $S_{a_2 \rightarrow a_1}(\omega) \approx -i\omega\sqrt{\mathcal{G}}/\Gamma_m$  (cf. SI), such that the product of gain and isolation bandwidth ( $\Gamma_m/\sqrt{\mathcal{G}}$ ) is  $\Gamma_m$ . Since the gain bandwidth is larger than the isolation bandwidth, there is large reverse gain off resonance [cf. Fig. 2(d)], and noise from cavity 2 dominates the noise spectral density at cavity 1 [cf. Fig. 2(f)]. With increasing effective mechanical linewidth  $\Gamma_m$  (through additional sideband cooling), the isolation bandwidth grows, suppressing reverse gain off resonance (cf. red (dashed) curve in Fig. 2 and Ref. [16]).

*Directional phase-sensitive amplifier (DPSA).*—We now turn to an implementation of a DPSA, which necessitates six drives. Essentially, we replace the amplifier interaction in the DPPA by a phase-sensitive quantum non-demolition (QND) interaction that couples one quadrature of cavity 2 to only one quadrature of the mechanical resonator [40, 41]. This can be done by choosing

$$\mathbf{G} = \frac{1}{2} \begin{pmatrix} e^{i\Phi/2} \sqrt{C_1\Gamma_{m,1}\kappa_1} & e^{-i\Phi/2} \sqrt{C_1\Gamma_{m,2}\kappa_1} \\ \sqrt{C_2\Gamma_{m,1}\kappa_2} & \sqrt{C_2\Gamma_{m,2}\kappa_2} \end{pmatrix}, \quad (10)$$

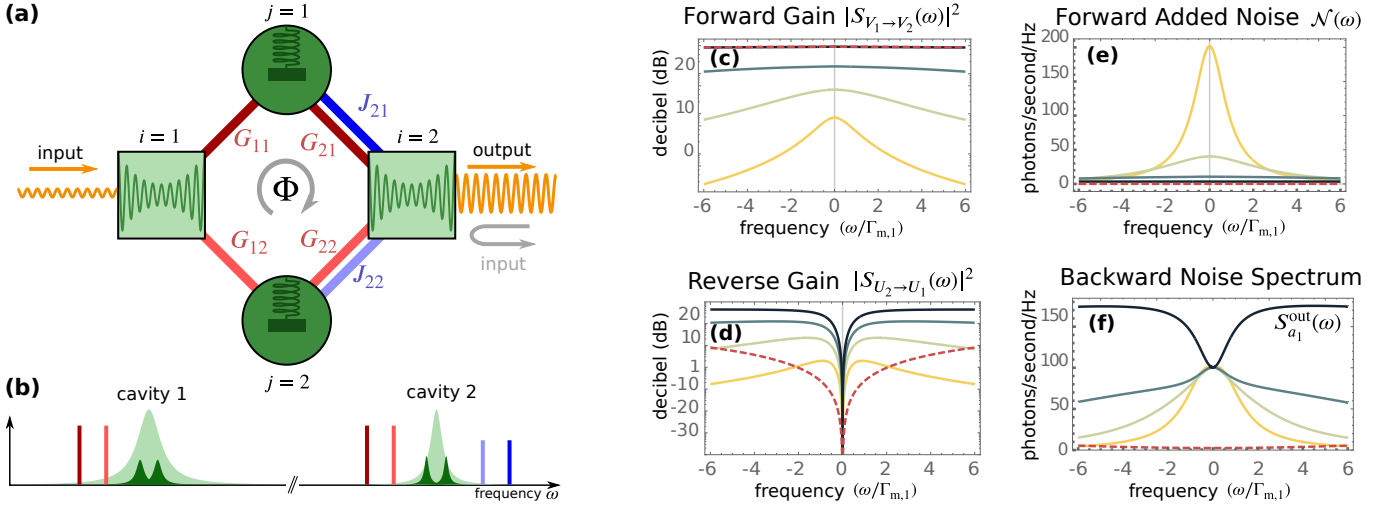


FIG. 3. (Color online.) The directional phase-sensitive amplifier (DPSA). **(a)** Model. Single red hopping interactions are impedance matched, double red-blue provide the phase-sensitive amplification. **(b)** Pump setup. Cavity 1 is pumped on the red sidebands of the mechanical resonators, whereas cavity 2 has pumps on the red and blue sidebands. In **(c-f)** we plot forward gain, reverse gain [cf. Eq. (7)], added noise [Eq. (9)], and the output noise fluctuation spectrum of cavity 1, all as functions of frequency in units of  $\Gamma_{m,1}$ , for cooperativities  $C_1 = \{1, 3, 10, 30\}$ ,  $C_2 = C_1^2$  (yellow to black, or light to dark). The parameters are the same as in Fig. 2. External sideband cooling with an auxiliary mode can achieve  $n_{m,j} \approx 0$ , without negatively affecting amplification properties, as described below. The red (dashed) curve in each plot illustrates this case, with  $C_1 = 30$  and effective parameters  $n_{\text{eff},i} = n_{m,i}(\Gamma_{m,i}/\Gamma_{\text{eff},i})$ ,  $\Gamma_{\text{eff},i} = 50\Gamma_{m,i}$ .

and the same  $\mathbf{J}$  as for the DPPA [Eq. (5)]. The coupling is illustrated in Fig. 3(a,b). Since the QND interaction requires couplings of matching strength, and we have chosen the two arms of the amplifier to be symmetric for simplicity, the six drives are parametrized by only two cooperativities. In the DPSA, we need to ensure that the signal quadrature we measure on one mechanical resonator agrees with the one on the other,  $\mu = \arg(G_{11}\chi_{m,1}(0)G_{21}/J_{21}) = \arg(\pm G_{12}\chi_{m,2}(0)G_{22}/J_{22})$ , and that the information emerges on the same cavity quadrature,  $\nu = \arg(G_{21}J_{21}) = \arg(\pm G_{22}J_{22})$ .  $\mu$  and  $\nu$  determine the quadratures involved in amplification. The two remaining phases are an arbitrary phase of the mechanical resonators, and the plaquette phase.

The isolation, detuning, and impedance-matching conditions are the same as for the DPPA, and we obtain our central result, the scattering matrix

$$\begin{pmatrix} U_{1,\text{out}} \\ V_{1,\text{out}} \\ U_{2,\text{out}} \\ V_{2,\text{out}} \end{pmatrix} = \begin{pmatrix} 0 & 0 & 0 & 0 \\ 0 & 0 & 0 & 0 \\ 0 & 0 & -1 & 0 \\ 0 & \sqrt{G} & 0 & -1 \end{pmatrix} \begin{pmatrix} U_{1,\text{in}} \\ V_{1,\text{in}} \\ U_{2,\text{in}} \\ V_{2,\text{in}} \end{pmatrix} + \frac{1}{\sqrt{2}} \begin{pmatrix} 1 & 0 & -1 & 0 \\ 0 & 1 & 0 & -1 \\ 0 & 0 & 0 & 0 \\ \sqrt{2F} & 0 & \sqrt{2F} & 0 \end{pmatrix} \begin{pmatrix} X_{1,\text{in}} \\ P_{1,\text{in}} \\ X_{2,\text{in}} \\ P_{2,\text{in}} \end{pmatrix}, \quad (11)$$

where we defined noise scattering intensity  $F \equiv \frac{4C_2}{C_1^2}$ , gain

$$G = \frac{8C_2(2C_1 - 1)}{C_1^2}, \quad (12)$$

mechanical  $X_i = (b_i + b_i^\dagger)/\sqrt{2}$ ,  $P_i = i(b_i^\dagger - b_i)/\sqrt{2}$ , and optical quadratures  $U_i = (a_i + a_i^\dagger)/\sqrt{2}$ ,  $V_i = i(a_i^\dagger - a_i)/\sqrt{2}$ .

The amplifier is phase-sensitive and directional, as only the phase quadrature of the second cavity,  $V_2$ , inherits the amplified signal from the phase quadrature of the first cavity,  $V_1$ . We calculate the noise added to the signal as before

$$\mathcal{N}_{\text{DPSA}} = \frac{n_{m,1} + n_{m,2} + 1}{2(2C_1 - 1)} + \frac{C_1}{8C_2} \frac{C_1}{2C_1 - 1} \left( n_{c,2} + \frac{1}{2} \right). \quad (13)$$

The crucial difference to the DPPA is that the noise stemming from reflection of fluctuations at cavity 2 can *also* be suppressed, such that in the limit  $C_2 \gg C_1 \gg 1$ , the added noise vanishes. Therefore, the DPSA can reach its quantum limit of zero added noise. The reverse noise on resonance is as before,  $S_{1,\text{DPSA}}^{\text{out}}(0) = S_{1,\text{DPPA}}^{\text{out}}(0)$ , and is discussed below.

To investigate the off-resonant behavior of the DPSA, we plot forward gain, reverse gain, added noise, and spectral noise density at cavity 1 in Fig. 3(c-f) at cooperativities  $C_1 = \{1, 3, 10, 30\}$ ,  $C_2 = C_1^2$ . Increasing  $C_1$  enhances bandwidth and gain [cf. Fig. 3(c)]. At the same time, the mechanical noise is suppressed [cf. Fig. 3(e)]. Close to resonance, the reverse scattering behaves the same as for the DPPA  $S_{a_2 \rightarrow a_1}(\omega) \approx -i\omega\sqrt{G}/\Gamma_m$  (cf. SI), and the same conclusions apply [cf. Fig. 3(d,f)]. In particular, the gain-isolation-bandwidth product is  $\Gamma_m$ . Forward and reverse gain are proportional to  $\sqrt{C_2}$ , implying an unlimited gain-bandwidth product (cf. SI). For equivalent mechanical resonators  $\Gamma_{m,1} = \Gamma_{m,2} = \Gamma_m$  and in the limit  $\kappa/\Gamma_m \gg \{1, C_1\}$ , the amplitude gain bandwidth of the DPSA is well approximated by  $\Gamma_{\text{gain}} = 2C_1\Gamma_m$ .

*Backward propagating noise and sideband cooling.*—The



noise emitted in the reverse direction is of central importance for directional amplifiers. For both DPPA and DPSA, the output noise spectral density of cavity 1 on resonance is  $S_{1,\text{DPSA}}^{\text{out}}(0) = S_{1,\text{DPPA}}^{\text{out}}(0) = (n_{m,1} + n_{m,2} + 1)/2$ . Due to impedance matching and directionality, fluctuations incident on the cavities do not appear in  $a_{1,\text{out}}$  [cf. Eqs. (7) and (11)]. Preserving the commutation relations of  $a_{1,\text{out}}$  implies that instead mechanical fluctuations have to appear in the output  $\sum_{j=1}^2 (|S_{b_i \rightarrow a_1}(0)|^2 - |S_{b_i^\dagger \rightarrow a_1}(0)|^2) = 1$ . The lowest possible value for  $S_{1,\text{out}}$  is  $1/2$ , can be attained for zero thermal noise quanta in the mechanical resonators.

However, even in state-of-the-art dilution refrigerators, such temperatures are out of reach. External sideband cooling with an auxiliary mode can achieve  $n_m \rightarrow 0$  [42–44], and has the additional benefit of enhancing mechanical linewidths [cf. red (dashed) curve in Figs. 2 and 3], as discussed below. Whilst this could be done with an additional cavity mode for each resonator, implementing a circuit with four cavity modes coupled to two mechanical resonators is a formidable technical challenge. A problem arises when cooling with only one additional mode, since it can lead to a coupling of the mechanical resonators via the extra cooling mode, thereby changing the topology of the system thus spoiling the directional amplifier. We show in the SI as part of the analysis of off-resonant terms that this can be mitigated by detuning each pump by several mechanical linewidths, making cooling with only one additional mode feasible.

**Conclusion.**—We have presented quantum-limited, non-reciprocal amplifiers using an optomechanical plaquette comprising two cavities and intermediate mechanical resonators [4, 5]. Such devices carry great promise, since they can be integrated into superconducting circuits and amplify near or at the quantum limit, whilst protecting the signal source.

**Acknowledgements.**—We are grateful to John Teufel, and in particular Anja Metelmann for insightful discussions and helpful comments. DM acknowledges support by the UK Engineering and Physical Sciences Research Council (EPSRC) under Grant No. EP/M506485/1. This work was supported by the SNF, the NCCR Quantum Science and Technology (QSIT), and the European Union’s Horizon 2020 research and innovation programme under grant agreement No 732894 (FET Proactive HOT). TJK acknowledges financial support from an ERC AdG (QuREM). AN holds a University Research Fellowship from the Royal Society and acknowledges support from the Winton Programme for the Physics of Sustainability.

---

[1] K. Gallo, G. Assanto, K. R. Parameswaran, and M. M. Fejer, *Applied Physics Letters* **79**, 314 (2001).  
 [2] J. Koch, A. A. Houck, K. L. Hur, and S. M. Girvin, *Physical Review A* **82**, 043811 (2010), arXiv:1006.0762.  
 [3] K. Fang, Z. Yu, and S. Fan, *Nature Photonics* **6**, 782 (2012).  
 [4] D. L. Sounas, C. Caloz, and A. Alù, *Nature Communications* **4**, 2407 (2013), arXiv:1011.1669.

[5] A. Kamal, J. Clarke, and M. H. Devoret, *Nature Physics* **7**, 311 (2011).  
 [6] C. G. Poulton, R. Pant, A. Byrnes, S. Fan, M. J. Steel, and B. J. Eggleton, *Optics Express* **20**, 21235 (2012).  
 [7] S. Longhi, *Optics Letters* **38**, 3570 (2013), arXiv:arXiv:1310.5001v1.  
 [8] K. Fang, Z. Yu, and S. Fan, *Physical Review B* **87**, 060301 (2013).  
 [9] D.-W. Wang, H.-T. Zhou, M.-J. Guo, J.-X. Zhang, J. Evers, and S.-Y. Zhu, *Physical Review Letters* **110**, 093901 (2013), arXiv:1204.0837.  
 [10] B. Abdo, K. Sliwa, S. Shankar, M. Hatridge, L. Frunzio, R. Schoelkopf, and M. Devoret, *Physical Review Letters* **112**, 167701 (2014), arXiv:1311.5345.  
 [11] K. M. Sliwa, M. Hatridge, A. Narla, S. Shankar, L. Frunzio, R. J. Schoelkopf, and M. H. Devoret, *Physical Review X* **5**, 041020 (2015), arXiv:1503.00209.  
 [12] F. Lecocq, L. Ranzani, G. A. Peterson, K. Cicak, R. W. Simmonds, J. D. Teufel, and J. Aumentado, *Physical Review Applied* **7**, 024028 (2017), arXiv:1612.01438.  
 [13] B. Abdo, K. Sliwa, L. Frunzio, and M. Devoret, *Physical Review X* **3**, 031001 (2013), arXiv:1302.4663.  
 [14] L. Ranzani and J. Aumentado, *New Journal of Physics* **16**, 103027 (2014), arXiv:1406.4922.  
 [15] L. Ranzani and J. Aumentado, *New Journal of Physics* **17**, 23024 (2015), arXiv:1406.4922v2.  
 [16] A. Metelmann and A. A. Clerk, *Physical Review X* **5**, 021025 (2015), arXiv:1502.07274.  
 [17] K. Fang, J. Luo, A. Metelmann, M. H. Matheny, F. Marquardt, A. A. Clerk, and O. Painter, *Nature Physics*, 1 (2017), arXiv:1608.03620.  
 [18] A. Kamal and A. Metelmann, arXiv:1607.06822.  
 [19] A. Metelmann and A. A. Clerk, *Physical Review A* **95**, 013837 (2017), arXiv:1610.06621.  
 [20] Z. Shen, Y.-L. Zhang, Y. Chen, C.-L. Zou, Y.-F. Xiao, X.-B. Zou, F.-W. Sun, G.-C. Guo, and C.-H. Dong, *Nature Photonics* **10**, 657 (2016), arXiv:1604.02297.  
 [21] F. Ruesink, M.-A. Miri, A. Alù, and E. Verhagen, *Nature Communications* **7**, 13662 (2016), arXiv:1607.07180.  
 [22] X.-W. Xu, Y. Li, A.-X. Chen, and Y.-X. Liu, *Physical Review A* **93**, 023827 (2016), arXiv:1511.05751.  
 [23] N. R. Bernier, L. D. Tóth, A. Koottandavida, A. Nunnenkamp, A. K. Feofanov, and T. J. Kippenberg, arXiv:1612.08223.  
 [24] G. A. Peterson, F. Lecocq, K. Cicak, R. W. Simmonds, J. Aumentado, and J. D. Teufel, arXiv:1703.05269.  
 [25] F. Massel, T. T. Heikkilä, J.-M. Pirkkalainen, S. U. Cho, H. Saloniemi, P. J. Hakonen, and M. A. Sillanpää, *Nature* **480**, 351 (2011), arXiv:1107.4903.  
 [26] A. Metelmann and A. A. Clerk, *Physical Review Letters* **112**, 133904 (2014), arXiv:1311.0273v1.  
 [27] A. Nunnenkamp, V. Sudhir, A. K. Feofanov, A. Roulet, and T. J. Kippenberg, *Physical Review Letters* **113**, 023604 (2014).  
 [28] L. D. Tóth, N. R. Bernier, A. Nunnenkamp, E. Glushkov, A. K. Feofanov, and T. J. Kippenberg, arXiv:1602.05180.  
 [29] J. Suh, A. J. Weinstein, C. U. Lei, E. E. Wollman, S. K. Steinke, P. Meystre, A. A. Clerk, and K. C. Schwab, *Science* **344**, 1262 (2014), arXiv:1312.4084.  
 [30] J.-M. Pirkkalainen, E. Damskägg, M. Brandt, F. Massel, and M. A. Sillanpää, *Physical Review Letters* **115**, 243601 (2015), arXiv:1507.04209.  
 [31] E. E. Wollman, C. U. Lei, A. J. Weinstein, J. Suh, A. Kronwald, F. Marquardt, A. A. Clerk, and K. C. Schwab, *Science* **349**, 952 (2015), arXiv:1507.01662.  
 [32] C. U. Lei, A. J. Weinstein, J. Suh, E. E. Wollman, A. Kronwald,

- F. Marquardt, A. A. Clerk, and K. C. Schwab, *Physical Review Letters* **117**, 100801 (2016), [arXiv:1605.08148](#).
- [33] A. A. Clerk, M. H. Devoret, S. M. Girvin, F. Marquardt, and R. J. Schoelkopf, *Reviews of Modern Physics* **82**, 1155 (2010), [arXiv:0810.4729](#).
- [34] M. Aspelmeyer, T. J. Kippenberg, and F. Marquardt, *Reviews of Modern Physics* **86**, 1391 (2014).
- [35] C. W. Gardiner and M. J. Collett, *Physical Review A* **31**, 3761 (1985).
- [36] C. Gardiner and P. Zoller, *Quantum Noise: A Handbook of Markovian and Non-Markovian Quantum Stochastic Methods with Applications to Quantum Optics*, Springer Series in Synergetics (Springer, 2004).
- [37] This condition ensures the modulus of the transmission amplitudes via resonator 1 and 2 coincide,  $|G_{11}J_{21}\chi_{m,1}(0)| = |G_{12}J_{22}\chi_{m,2}(0)|$ , which is needed for complete destructive interference.
- [38] Private communication with Anja Metelmann. Note that disabling one arm of the circuit,  $G_{21} = J_{22} = 0$ , choosing  $G_{11} = J_{12}$ , and setting the detuning to zero, a reciprocal amplifier with unlimited gain-bandwidth product is obtained [26].
- [39] C. M. Caves, *Physical Review D* **26**, 1817 (1982).
- [40] V. B. Braginsky, Y. I. Vorontsov, and K. S. Thorne, *Science* **209**, 547 (1980).
- [41] A. A. Clerk, F. Marquardt, and K. Jacobs, *New Journal of Physics* **10**, 095010 (2008), [arXiv:0802.1842](#).
- [42] J. D. Teufel, T. Donner, D. Li, J. W. Harlow, M. S. Allman, K. Cicak, A. J. Sirois, J. D. Whittaker, K. W. Lehnert, and R. W. Simmonds, *Nature* **475**, 359 (2011), [arXiv:1103.2144](#).
- [43] J. Chan, T. P. M. Alegre, A. H. Safavi-Naeini, J. T. Hill, A. Krause, S. Gröblacher, M. Aspelmeyer, and O. Painter, *Nature* **478**, 89 (2011), [arXiv:1106.3614](#).
- [44] R. Rivière, S. Deléglise, S. Weis, E. Gavartin, O. Arcizet, A. Schliesser, and T. J. Kippenberg, *Physical Review A* **83**, 063835 (2011), [arXiv:1011.0290](#).
-

## Supplemental Materials: Quantum-limited directional amplifiers with optomechanics

### MOST GENERAL TIME-INDEPENDENT HAMILTONIAN

For an introduction to optomechanics and input-output theory, we refer to Refs. [S1, S2]. The optomechanical Hamiltonian for the plaquette is given by ( $\hbar = 1$ )

$$H_{\text{sys}} = \sum_i \omega_{c,i} a_i^\dagger a_i + \Omega_i b_i^\dagger b_i - \sum_{ij} g_{0,ij} a_i^\dagger a_i (b_j + b_j^\dagger). \quad (\text{S1})$$

$g_{0,ij}$  is the bare coupling between the  $i$ th cavity and the  $j$ th mechanical resonator. Each cavity is driven by up to four lasers, at frequencies  $\omega_{c,i} \pm (\Omega_j + \delta_j)$ , i.e., on the red and blue motional sidebands due to the mechanical resonators, as illustrated in Fig. 1 in the main text. The drives generate coherent states in the cavities, such that the annihilation operators for the cavity modes can be written as a sum of coherent parts and vacuum fluctuations  $\delta \hat{a}_i$

$$\hat{a}_i = e^{-i\omega_{c,i}t} \left( \alpha_{i1+} e^{-i(\Omega_1 + \delta_1)t} + \alpha_{i1-} e^{i(\Omega_1 + \delta_1)t} + \alpha_{i2+} e^{-i(\Omega_2 + \delta_2)t} + \alpha_{i2-} e^{i(\Omega_2 + \delta_2)t} + \delta \hat{a}_i \right), \quad (\text{S2})$$

where  $\alpha_i$  are c-numbers that describe the coherent state, and  $\delta \hat{a}_i$  is a bosonic operator with zero mean. In the following, we will rename  $\delta \hat{a}_i \rightarrow \hat{a}_i$  for a cleaner notation, and drop the hats. Going into a rotating frame with respect to

$$H_0 = \sum_j (\Omega_j + \delta_j) b_j^\dagger b_j + \sum_i \omega_{c,i} a_i^\dagger a_i, \quad (\text{S3})$$

and using Eq. (S2), the time-independent Hamiltonian [Eq. (1) in the main text] corresponds to all time-independent (off-resonant) terms in

$$H_{\text{rotating frame}} = - \sum_j \delta_j b_j^\dagger b_j - \sum_{ij} g_{0,ij} a_i^\dagger a_i \left[ b_j e^{-i(\Omega_j + \delta_j)t} + b_j^\dagger e^{i(\Omega_j + \delta_j)t} \right]. \quad (\text{S4})$$

In the main text, we neglect all time-dependent terms for simplicity. When calibrating pumps and phases, their effect will likely have to be included. We analyze them below, but the upshot is that to a very good approximation, off-resonant terms amount to a change of effective parameters, such that the description in the main text is still valid. We describe the system with input-output theory and quantum Langevin equations [S1–S3]

$$b_j(\omega) = \chi_{m,j}(\omega) \left\{ i \sum_{i=1}^2 \left[ a_i(\omega) G_{ij}^* + a_i^\dagger(\omega) J_{ij} \right] + b_{j,\text{in}}(\omega) \right\}, \quad (\text{S5a})$$

$$a_i(\omega) = \chi_{c,i}(\omega) \left\{ i \sum_{j=1}^2 \left[ G_{ij} b_j(\omega) + J_{ij} b_j^\dagger(\omega) \right] + a_{i,\text{in}}(\omega) \right\} \quad (\text{S5b})$$

with susceptibilities  $\chi_{m,i}(\omega) = [\Gamma_{m,i}/2 - i(\omega + \delta_i)]^{-1}$  and  $\chi_{c,i}(\omega) = [\kappa_i/2 - i\omega]^{-1}$ , and mechanical (cavity) dissipation rates  $\Gamma_{m,i}$  ( $\kappa_i$ ). The mechanical (cavity) input noise operators  $b_{i,\text{in}}$  ( $a_{i,\text{in}}$ ) are assumed to have bosonic commutation relations and delta-correlated noise  $\langle b_{i,\text{in}}^\dagger(t) b_{j,\text{in}}(t') \rangle = \delta_{ij} n_{m,i} \delta(t - t')$ ,  $\langle a_{i,\text{in}}^\dagger(t) a_{j,\text{in}}(t') \rangle = \delta_{ij} n_{c,i} \delta(t - t')$ . In order to obtain a description only in terms of the microwave modes, we eliminate the mechanical degrees of freedom in Eq. (S5b) with Eq. (S5a). This yields Eq. (3) in the main text.

The coupling matrices  $i\mathbf{T}_{ij}$ , defined in Eq. 3, exhibit the symmetry

$$\mathbf{T}_{ij}(\omega) = \sigma_1 \mathbf{T}_{ij}^*(-\omega) \sigma_1, \quad (\text{S6})$$

since we are using both annihilation operators and their conjugates. The minus sign in the frequency is due to our choice of Fourier transform,  $[a_i(\omega)]^\dagger = a_i^\dagger(-\omega)$ . This is the only symmetry, since we know that there are 8 free complex parameters (the 8 driving amplitudes), and  $T$  has  $4^2 = 16$  complex entries.

### MORE DETAILS ON DETUNING CHOICES

Isolation can be achieved when  $\mathbf{T}_{12} = 0$ , i.e., the first cavity is decoupled from the second, but  $\mathbf{T}_{21} \neq 0$ , i.e., the second cavity is coupled to the first. For the DPPA, these requirements turn into

$$[i\mathbf{T}_{12}]_{12} = \chi_{m,1}(0) G_{11} J_{12} + \chi_{m,2}(0) G_{21} J_{22} = 0, \quad (\text{S7a})$$

$$[i\mathbf{T}_{21}]_{12} = \chi_{m,1}^*(0) G_{11} J_{12} + \chi_{m,2}^*(0) G_{21} J_{22} \neq 0. \quad (\text{S7b})$$

For the choice of driving strengths in the main text Eq. (5) (repeated here for convenience)

$$\mathbf{G} = \frac{1}{2} \begin{pmatrix} e^{\frac{i\Phi}{2}} \sqrt{C_1 \Gamma_{m,1} \kappa_1} & 0 \\ e^{-\frac{i\Phi}{2}} \sqrt{C_1 \Gamma_{m,2} \kappa_1} & 0 \end{pmatrix}, \quad \mathbf{J} = \frac{1}{2} \begin{pmatrix} 0 & \sqrt{C_2 \Gamma_{m,1} \kappa_2} \\ 0 & \sqrt{C_2 \Gamma_{m,2} \kappa_2} \end{pmatrix}, \quad (\text{S8})$$

we find

$$0 = i\Gamma_{m,1}\Gamma_{m,2} + 2\delta_1\Gamma_{m,2} + e^{i\Phi}(i\Gamma_{m,1}\Gamma_{m,2} + 2\delta_2\Gamma_{m,1}), \quad (\text{S9a})$$

$$0 \neq i\Gamma_{m,1}\Gamma_{m,2} + 2\delta_1\Gamma_{m,2} + e^{-i\Phi}(i\Gamma_{m,1}\Gamma_{m,2} + 2\delta_2\Gamma_{m,1}). \quad (\text{S9b})$$

Taking the modulus, we find that isolation requires

$$\frac{\delta_1^2}{\Gamma_{m,1}^2} = \frac{\delta_2^2}{\Gamma_{m,2}^2}. \quad (\text{S10})$$

Note that sending  $\Phi \rightarrow -\Phi$  interchanges the two equations in Eq. (S9), which means that isolation now occurs in the opposite direction. In order to avoid “double isolation”, where the forward and backward transmission vanish at the same plaquette phase (as per the previous sentence, this occurs for  $\Phi = 0$  or  $\Phi = \pi$ ), we need  $\delta_1/\Gamma_{m,1} \neq \delta_2/\Gamma_{m,2}$ . The phase at which isolation is obtained is given in Eq. (6) in the main text.

For these choices, the scattering amplitude from  $a_{1,\text{in}}$  to  $a_{1,\text{out}}$  (reflection) is given by

$$S_{a_1 \rightarrow a_1}(0) = \frac{4C_1}{4\delta^2 + 2C_1 + 1} - 1. \quad (\text{S11})$$

Impedance matching is attained at zero reflection, namely when

$$\delta = \sqrt{2C_1 - 1}/2, \quad (\text{S12})$$

the same as in Ref. [S4].

### DIRECTIONAL PHASE-INSENSITIVE AMPLIFIER WITH ONLY BLUE TONES

Here we analyze the optomechanical plaquette with only pumps on the upper motional sidebands. While directional phase-insensitive amplification is still possible, the signal cannot be impedance matched. We choose coupling amplitudes as follows

$$\mathbf{G} = 0, \quad \mathbf{J} = \frac{1}{2} \begin{pmatrix} e^{\frac{i\Phi}{2}} \sqrt{C_1 \Gamma_{m,1} \kappa_1} & e^{-\frac{i\Phi}{2}} \sqrt{C_1 \Gamma_{m,2} \kappa_1} \\ \sqrt{C_2 \Gamma_{m,1} \kappa_2} & \sqrt{C_2 \Gamma_{m,2} \kappa_2} \end{pmatrix}. \quad (\text{S13})$$

The analysis proceeds similarly to the DPPA in the main text.  $\Phi$  is the only physically relevant phase. We choose the same detuning parametrisation as before  $\delta_1 = \delta\Gamma_{m,1}$  and  $\delta_2 = -\delta\Gamma_{m,2}$ , in which case the plaquette phase takes the same form as before [Eq. (6)]. However, if we look at the optical scattering matrix, we find

$$\begin{pmatrix} a_{1,\text{out}} \\ a_{2,\text{out}} \end{pmatrix} = \begin{pmatrix} -1 - \frac{4C_1}{4\delta^2 + 1 - 2C_1} & 0 \\ \frac{-16\delta\sqrt{C_1 C_2}(4\delta^2 + 1)}{(4\delta^2 - 2C_1 + 1)(4\delta^2 - 2C_2 + 1)} & -1 - \frac{4C_2}{4\delta^2 - 2C_2 + 1} \end{pmatrix} \begin{pmatrix} a_{1,\text{in}} \\ a_{2,\text{in}} \end{pmatrix} + \text{mechanical noise}. \quad (\text{S14})$$

The cooperativities are obey  $4\delta^2 + 1 > C_i > 0$ , where the first condition is required for stability and the second arises by definition, such that impedance matching is not possible, and input will be reflected and amplified. This property is already highly undesirable in a directional amplifier, since the main point of a directional amplifier is protection of the system that emits the signal.

Amplification is obtained if either or both of the cooperativities approach  $2\delta^2 + 1/2$ .  $C_1 \rightarrow 2\delta^2 + 1/2$  leads to a lot of noise being emitted from cavity 1, both due to the reflection and due to amplified mechanical noise (not shown above). Hence, we consider  $C_2 = 2\delta^2 + 1/2 - \epsilon$ , for some small  $\epsilon > 0$ , and  $C_1 = 1/2$ . For  $\delta^2 \gg \epsilon$ , we can write

$$\begin{pmatrix} a_{1,\text{out}} \\ a_{2,\text{out}} \end{pmatrix} = \frac{\sqrt{4\delta^2 + 1}}{\sqrt{2}\delta} \begin{pmatrix} -\frac{1}{2\delta} & \frac{1}{2\delta} \\ -\frac{\delta(2\delta+i)+1}{\epsilon} & \frac{\delta(2\delta-i)+1}{\epsilon} \end{pmatrix} \begin{pmatrix} b_{1,\text{in}} \\ b_{2,\text{in}} \end{pmatrix} - \begin{pmatrix} 1 + \frac{1}{2\delta^2} & 0 \\ \frac{4\delta^2+1}{\delta\epsilon} & \frac{4\delta^2+1}{\epsilon} \end{pmatrix} \begin{pmatrix} a_{1,\text{in}} \\ a_{2,\text{in}} \end{pmatrix}. \quad (\text{S15})$$



For large  $\delta$ , the signal source is only subject to the reflected signal and noise at cavity 1, leading to the approximate scattering matrix

$$\begin{pmatrix} a_{1,\text{out}} \\ a_{2,\text{out}} \end{pmatrix} = \frac{\delta^2}{\epsilon} \begin{pmatrix} 0 & 0 \\ -1 & 1 \end{pmatrix} \begin{pmatrix} b_{1,\text{in}} \\ b_{2,\text{in}} \end{pmatrix} + \begin{pmatrix} -1 & 0 \\ \frac{4\delta}{\epsilon} & \frac{4\delta^2}{\epsilon} \end{pmatrix} \begin{pmatrix} a_{1,\text{in}} \\ a_{2,\text{in}} \end{pmatrix}. \quad (\text{S16})$$

The suppression of mechanical noise works well for cavity 1, but cavity 2, where the signal emerges, is subject to amplified mechanical noise. As a consequence, the amplification is not quantum-limited, in addition to the lack of impedance matching. Interchanging  $C_1 \leftrightarrow C_2$  leads to

$$\begin{pmatrix} a_{1,\text{out}} \\ a_{2,\text{out}} \end{pmatrix} = \frac{4\delta}{\sqrt{2}\epsilon} \begin{pmatrix} -1 & 1 \\ -1 & 1 \end{pmatrix} \begin{pmatrix} b_{1,\text{in}} \\ b_{2,\text{in}} \end{pmatrix} + \begin{pmatrix} -\frac{4\delta^2}{\epsilon} & 0 \\ -\frac{4\delta}{\epsilon} & -1 \end{pmatrix} \begin{pmatrix} a_{1,\text{in}} \\ a_{2,\text{in}} \end{pmatrix}, \quad (\text{S17})$$

i.e., the amplification is quantum-limited, but the signal source is subject to amplified mechanical and optical noise.

### BANDWIDTH AND GAIN-BANDWIDTH PRODUCT OF DPPA

For  $\Gamma_{m,1} = \Gamma_{m,2} = \Gamma_m$  and  $\kappa_1 = \kappa_2 = \kappa$ , the scattering amplitudes are

$$S_{a_2^\dagger \rightarrow a_1}(\omega) = (-i\omega) \sqrt{2C_2(2C_1 - 1)} / \mathcal{A}(\omega), \quad (\text{S18a})$$

$$S_{a_1 \rightarrow a_2^\dagger}(\omega) = \sqrt{2C_2(2C_1 - 1)}(i\omega - \Gamma_m) / \mathcal{A}(\omega), \quad (\text{S18b})$$

with

$$\mathcal{A}(\omega) = (\Gamma_m \kappa^2)^{-1} \{ i\omega(\Gamma_m - i\omega)(\kappa - 2i\omega)^2 + C_1 \Gamma_m (\kappa - 2i\omega) [\Gamma_m \kappa - i(\Gamma_m + \kappa)\omega] + C_2 \Gamma_m \kappa [2\omega^2 + i(\Gamma_m + \kappa)\omega - \Gamma_m \kappa] \}. \quad (\text{S19})$$

For the gain-bandwidth product, we are most interested in the limit of large gain,  $\mathcal{G} \gg 1$ . This implies  $(C_1 - C_2)^2 \ll 4C_1 C_2 < 2(C_1 + C_2)^2$ . We further assume  $C_1 \gg \{1, \Gamma_m/\kappa, \kappa/\Gamma_m\}$ , in which case the first term in the curly brackets in Eq. (S19) can be neglected. In this approximation,

$$\mathcal{A}(\omega) = \kappa^{-2} \{ (C_1 + C_2) [-i\omega \Gamma_m (\kappa - i\omega)] + (C_1 - C_2) [\Gamma_m (\kappa - i\omega)^2 - i\kappa \omega (\kappa - 2i\omega)] \}. \quad (\text{S20})$$

The bandwidth is approximated by the smallest  $|\omega|$  at which  $2|\mathcal{A}(0)|^2 = |\mathcal{A}(\omega)|^2$ . Expanding both square brackets to first order in  $\omega$ , we find that the amplitude bandwidth is approximately

$$\Gamma = \frac{2\Gamma_m(C_1 - C_2)}{2C_1 \frac{\Gamma_m}{\kappa} + \left(1 + \frac{\Gamma_m}{\kappa}\right)(C_1 - C_2)}. \quad (\text{S21})$$

The gain-bandwidth product  $P \equiv \Gamma \sqrt{\mathcal{G}}$  is

$$P = \frac{2\Gamma_m \sqrt{4C_1 C_2}}{2C_1 \frac{\Gamma_m}{\kappa} + \left(1 + \frac{\Gamma_m}{\kappa}\right)(C_1 - C_2)}. \quad (\text{S22})$$

In the limit of large gain, with  $C_2 \rightarrow C_1$  and  $2C_1 \gg C_1 - C_2$ ,  $P$  tends to  $2\kappa$ .

We will now analyze the limits  $\kappa \gg \Gamma_m$  and  $\kappa \ll \Gamma_m$ , but note that they are only valid as long as  $C_1$  is smaller than the ratio of  $\kappa/\Gamma_m$  and  $\Gamma_m/\kappa$ . In the limit  $\kappa/\Gamma_m \gg \{1, C_1, C_2\}$ , we obtain

$$\mathcal{A}(\omega) \approx (\Gamma_m - i\omega) \Gamma_m^{-1} [\Gamma_m(C_1 - C_2) + i\omega], \quad (\text{S23})$$

which yields an amplitude bandwidth

$$\Gamma = 2(C_1 - C_2) \Gamma_m \quad (\text{S24})$$

and the intensity bandwidth  $\Gamma/2$ . The gain-bandwidth product, defined as  $P \equiv \Gamma \sqrt{\mathcal{G}}$  evaluates to

$$P = 2\sqrt{4C_1 C_2} \Gamma_m. \quad (\text{S25})$$

This implies that the gain-bandwidth product  $P$  increases with gain. When  $C_1\Gamma_m \sim \kappa$  the approximation above breaks down.

In the opposite limit,  $\kappa \ll \Gamma_m$ , we instead have

$$\mathcal{A}(\omega) \approx \kappa^{-2}\Gamma_m(\kappa - i\omega)C_1^2[\kappa(C_1 - C_2)/(2C_1) - i\omega], \quad (\text{S26})$$

which implies that the bandwidth is close to  $\kappa(C_1 - C_2)/C_1$  and thus  $P \approx \kappa\sqrt{4C_2/C_1}$ . For large gain,  $P \approx 2\kappa$ , as before.

The isolation bandwidth must be calculated separately. It is the range of frequencies over which sufficient isolation is attained. What sufficient means has to be decided depending on the purpose. Close to  $\omega = 0$ , to lowest order in  $\omega$ , the reverse gain departs linearly from zero, namely

$$S_{a_2^\dagger \rightarrow a_1}(\omega) = -i\omega \frac{\sqrt{2C_2(2C_1 - 1)}}{\Gamma_m(C_1 - C_2)} + \mathcal{O}(\omega^2) = -i\omega\sqrt{\mathcal{G}}/\Gamma_m + \mathcal{O}(\omega^2). \quad (\text{S27})$$

Thus, the isolation bandwidth is of order  $\Gamma_m/\sqrt{\mathcal{G}}$ , independent of  $\kappa$ .

### BANDWIDTH AND GAIN-BANDWIDTH PRODUCT OF DPSA

For the DPSA as discussed in the main text, we obtain

$$S_{a_1 \rightarrow a_2^\dagger}(\omega) = \sqrt{2C_2(2C_1 - 1)}(i\omega - \Gamma_m)/B(\omega), \quad (\text{S28a})$$

$$S_{a_2^\dagger \rightarrow a_1}(\omega) = \sqrt{2C_2(2C_1 - 1)}(-i\omega)/B(\omega), \quad (\text{S28b})$$

$$\text{with } B(\omega) = (\Gamma_m\kappa^2)^{-1}(\kappa - i\omega)\{C_1\Gamma_m[\Gamma_m\kappa - i\omega(\Gamma_m + \kappa)] - (\kappa - 2i\omega)i\omega(\Gamma_m - i\omega)\}. \quad (\text{S28c})$$

Here, since both  $S_{2 \rightarrow 1} \propto \sqrt{C_2}$  and  $S_{1 \rightarrow 2} \propto \sqrt{C_2}$ , we can immediately conclude that the bandwidth is independent of the gain, and the gain-bandwidth product therefore unlimited.

For  $\{C_1\omega, C_1\Gamma_m\} \ll \kappa$ , we find

$$B(\omega) \approx (\Gamma_m - i\omega)\Gamma_m^{-1}(C_1\Gamma_m - i\omega), \quad (\text{S29})$$

and therefore

$$S_{1 \rightarrow 2}(\omega) \approx \frac{\sqrt{2C_2(2C_1 - 1)}\Gamma_m}{-(C_1\Gamma_m - i\omega)}, \quad S_{2 \rightarrow 1}(\omega) \approx \frac{\sqrt{2C_2(2C_1 - 1)}i\omega\Gamma_m}{-(\Gamma_m - i\omega)(C_1\Gamma_m - i\omega)}, \quad (\text{S30})$$

such that the gain bandwidth  $\Gamma_{1 \rightarrow 2} = 2C_1\Gamma_m$ .

To gain information about the departure from isolation, we expand the reverse gain around  $\omega = 0$ . To first order (note that we do *not* assume  $\{C_1\omega, C_1\Gamma_m\} \ll \kappa$  here)

$$S_{2 \rightarrow 1}(\omega) = -i\omega \frac{\sqrt{2C_2(2C_1 - 1)}}{C_1\Gamma_m} + \mathcal{O}(\omega^2) = -i\omega\sqrt{\mathcal{G}}/\Gamma_m + \mathcal{O}(\omega^2). \quad (\text{S31})$$

Thus, the isolation bandwidth is again of order  $\Gamma_m/\sqrt{\mathcal{G}}$  (but note that  $\mathcal{G}$  takes different forms for DPSA and DPPA), independent of  $\kappa$ .

### OFF-RESONANT TERMS AND OFF-RESONANT COOLING

There are two kinds of off-resonant terms contained in Eq. (S4). One are ‘‘counterrotating terms’’, with a time-dependence  $\mathcal{O}(2\Omega_i)$ . Those will almost always be negligible. However, the off-resonant terms rotating at frequency  $\Omega = \Omega_2 + \delta_2 - \Omega_1 - \delta_1$  can have an appreciable effect [S4, S5]. Their Hamiltonian is

$$\begin{aligned} H_{\text{off-resonant}}(t) &= - \sum_i a_i^\dagger \left[ g_{0,i2}\alpha_{i1} + b_2^\dagger e^{i\Omega t} + g_{0,i2}\alpha_{i1} + b_2 e^{-i\Omega t} + g_{0,i1}\alpha_{i2} + b_1^\dagger e^{-i\Omega t} + g_{0,i1}\alpha_{i2} + b_1 e^{i\Omega t} \right] + \text{H.c.} \\ &= - \sum_i a_i^\dagger \left[ e^{i\Omega t} \left( \tilde{J}_{i2}b_2^\dagger + \tilde{G}_{i1}b_1 \right) + e^{-i\Omega t} \left( \tilde{G}_{i2}b_2 + \tilde{J}_{i1}b_1^\dagger \right) \right] + \text{H.c.}, \end{aligned} \quad (\text{S32})$$

where  $\tilde{G}_{i1} = G_{i2}g_{0,i1}/g_{0,i2}$  (and the same for  $G \leftrightarrow J$  and  $1 \leftrightarrow 2$ ). Including  $H_{\text{off-resonant}}$ , the Hamiltonian is no longer time-independent, but rather periodic, with period  $2\pi/\Omega$ . The resulting explicitly time-dependent Langevin equations can be mapped to stationary ones by use of a Floquet formalism [S6, S7], where we write system operators as Fourier series, for instance  $b(t) = \sum_n \exp(in\Omega t)b^{(n)}(t)$ . We obtain Langevin equations without explicit time-dependence (diagonal in frequency space)

$$\chi_{m,j}^{-1}(\omega - n\Omega)b_j^{(n)}(\omega) = i \sum_{i=1}^2 \left( a_i^{(n)} G_{ij}^* + a_i^{(n)\dagger} J_{ij} \right) + \delta_{n,0} \sqrt{\Gamma_{m,j}} b_{j,\text{in}} + i \sum_{i=1}^2 \left( a_i^{(n\pm 1)} \tilde{G}_{ij}^* + a_i^{(n\pm 1)\dagger} \tilde{J}_{ij} \right), \quad (\text{S33a})$$

$$\chi_{c,i}^{-1}(\omega - n\Omega)a_i^{(n)}(\omega) = i \sum_{j=1}^2 \left( G_{ij} b_j^{(n)} + J_{ij} b_j^{(n)\dagger} \right) + \delta_{n,0} \sqrt{\kappa_i} a_{i,\text{in}} + i \left( \tilde{J}_{i2} b_2^{(n-1)\dagger} + \tilde{G}_{i1} b_1^{(n-1)} + \tilde{G}_{i2} b_2^{(n+1)} + \tilde{J}_{i1} b_1^{(n+1)\dagger} \right), \quad (\text{S33b})$$

where in Eq. (S33)(a),  $j = 1$  corresponds to the  $+$ -sign and  $j = 2$  to the  $-$ -sign. Note that in our conventions  $[b^{(n)}(\omega)]^\dagger = b^{(-n)}(-\omega)$ . In principle, Eqs. (S33) constitute an infinitely large set of coupled linear equations (equivalently, an infinitely large matrix to invert). However, the coupling between different Fourier modes is suppressed by the mechanical and optical susceptibilities. In particular, the mechanical susceptibilities are strongly peaked ( $\Gamma_{m,i} \ll \Omega$ ), such that it is a good approximation to let  $b_j^{(n \neq 0)} = 0$ . Since in this approximation  $b_j = b_j^{(0)}$ , we will omit the superscript (0) for  $b$  in the following. Another consequence of the approximation is  $a_i^{(n)} = 0$  for  $|n| > 1$ .

We can think of  $a_i^{(\pm 1)}$  as four extra, “virtual” modes, as is done in Ref. [S4]. They are given through

$$a_i^{(1)}(\omega) = i \chi_{c,i}(\omega - \Omega) \left[ \tilde{J}_{i2} b_2^\dagger(\omega) + \tilde{G}_{i1} b_1(\omega) \right], \quad (\text{S34a})$$

$$a_i^{(-1)}(\omega) = i \chi_{c,i}(\omega + \Omega) \left[ \tilde{J}_{i1} b_1^\dagger(\omega) + \tilde{G}_{i2} b_2(\omega) \right], \quad (\text{S34b})$$

whence we write down the new equation of motion for  $b$  in Fourier space, e.g.,

$$\chi_{m,1}^{-1}(\omega) b_1(\omega) = i \sum_i \left[ G_{i1}^* a_i^{(0)} + J_{i1} a_i^{(0)\dagger} \right] + \sqrt{\Gamma_{m,1}} b_{1,\text{in}} - \sum_i \chi_{c,i}(\omega - \Omega) \left[ (|\tilde{G}_{i1}|^2 - |\tilde{J}_{i1}|^2) b_1 + (\tilde{G}_{i1}^* \tilde{J}_{i2} - \tilde{J}_{i1} \tilde{G}_{i2}^*) b_2^\dagger \right]. \quad (\text{S35})$$

The two types of terms that appear due to the off-resonant terms is one proportional to  $b_1$  that describes off-resonant cooling or heating, which can be incorporated into the susceptibility of the mechanical resonator, but also one that couples the first mechanical resonator to the second. The latter process only occurs when there is a drive on the red sideband of one resonator and one on the blue sideband of the other resonator. This is most easily understood when looking for example at the process underlying the term  $\chi_{m,1}(\omega - \Omega) b_2^\dagger \tilde{G}_{i1}^* \tilde{J}_{i2}$ .  $\tilde{J}_{i2}$  is an interaction that creates a phonon in resonator 2 and a photon in cavity 1, but the process is off-resonant, meaning that the frequency of the photon created is approximately  $\omega_{c,1} - \Omega$ .  $\tilde{G}_{i1}$  shifts the frequencies the other way, such that this term mediates a resonant interaction between the mechanical resonators, with an off-resonant intermediate state. In contrast,  $\tilde{J}_{i1}$  would create a phonon in resonator 1 and a photon in cavity at frequency  $\omega_{c,1} + \Omega$ . Thus the term  $\tilde{J}_{i1} \tilde{J}_{i2}$  would produce a phonon with frequency  $\Omega_1 - 2\Omega$ , a process that is strongly suppressed.

The spurious coupling between the resonators trivially vanishes in four-tone schemes, where one of  $G_{ij}$  or  $J_{ij}$  is zero for all  $i, j$ . For more tones, we have to find  $\tilde{G}_{i1}^* \tilde{J}_{i2} - \tilde{J}_{i1} \tilde{G}_{i2}^* = G_{i1}^* J_{i2} - J_{i1} G_{i2}^*$ . This vanishes for the DPSA, since in the case  $i = 1$ , there are only red drives, and for  $i = 2$ , the coupling strengths are the same  $J_{2j} = G_{2j}$  [see Eq. (10) in the main text]. Thus we can eliminate the off-resonant Fourier modes and write their effect as a self energy that modifies the susceptibility  $\chi_{m,i}^{-1}(\omega) \rightarrow \chi_{m,i}^{-1}(\omega) + \Sigma_1(\omega)$ , with

$$\Sigma_1(\omega) = \sum_i \left( \frac{g_{0,i1}}{g_{0,i2}} \right)^2 \chi_{c,i}(\omega - \Omega) (|G_{i2}|^2 - |J_{i2}|^2) \quad (\text{S36})$$

(for  $b_2$ , we do  $1 \leftrightarrow 2$ ). For the DPPA, we obtain

$$\begin{aligned} \Sigma_1^{\text{DPPA}} &= \left( \frac{g_{0,11}}{g_{0,12}} \right)^2 \chi_{c,1}(\omega - \Omega) \frac{C_1 \Gamma_{m,2} \kappa_1}{4} - \left( \frac{g_{0,21}}{g_{0,22}} \right)^2 \chi_{c,2}(\omega - \Omega) \frac{C_2 \Gamma_{m,2} \kappa_2}{4}, \\ \Sigma_2^{\text{DPPA}} &= \left( \frac{g_{0,12}}{g_{0,11}} \right)^2 \chi_{c,1}(\omega - \Omega) \frac{C_1 \Gamma_{m,1} \kappa_1}{4} - \left( \frac{g_{0,22}}{g_{0,21}} \right)^2 \chi_{c,2}(\omega - \Omega) \frac{C_2 \Gamma_{m,1} \kappa_2}{4}, \end{aligned} \quad (\text{S37})$$

whereas for the DPSA, the self-energies read

$$\begin{aligned}\Sigma_1^{\text{DPSA}} &= \left( \frac{g_{0,11}}{g_{0,12}} \right)^2 \chi_{c,1}(\omega - \Omega) \frac{C_1 \Gamma_{m,2} \kappa_1}{4}, \\ \Sigma_2^{\text{DPSA}} &= \left( \frac{g_{0,12}}{g_{0,11}} \right)^2 \chi_{c,1}(\omega - \Omega) \frac{C_1 \Gamma_{m,1} \kappa_1}{4}.\end{aligned}\quad (\text{S38})$$

Eqs. (S38) do not have a contribution from the drives on the second cavity, because the blue and red drives are balanced, such that the dynamical backaction cancels.

In the end, in an approximation where we neglect the frequency dependence of the self energies [i.e.,  $\chi_{c,i} \approx (\kappa_i/2 + i\Omega)^{-1}$ ], which is valid for small frequencies around resonance  $\omega \ll \Omega, \kappa_i$ , the effect of the complex self-energies can be subsumed as a change of damping and detuning parameters.

We stress again that the other important conclusion from this analysis is that the off-resonant terms do not change the topology of the circuit, neither in the DPPA nor in the DPSA, such that the theory presented in the main text applies to a very good approximation. The embedding into a Floquet ansatz explains how the extra modes and their properties arise in the description of Ref. [S4].

The above calculation can be repeated for the proposed off-resonant cooling with a third cavity mode. This involves two drives detuned from the sidebands of the mechanical resonator (or one drive roughly in the middle of the two sidebands). For instance, consider pumps at frequencies  $\omega_{c,3} - \Omega_j + \Delta_j$ , where  $\omega_{c,3}$  is the frequency of the third cavity mode,  $\Delta_1 = \Delta$ ,  $\Delta_2 = -\Delta$ , and  $\Delta \gg \Gamma_{m,j}$ . This leads to similar off-resonant terms as above, namely,

$$H_{\text{cool}} = -a_3^\dagger (e^{-i\Delta t} G_{31} b_1 + e^{i\Delta t} G_{32} b_2) + \text{H.c.} \quad (\text{S39})$$

This adds another contribution to the self-energy, similar to above

$$\Sigma_j^{\text{cool}}(\omega) = \chi_{c,3}(\omega) |G_{3j}|^2 \approx \frac{2}{\kappa_3} |G_{3j}|^2. \quad (\text{S40})$$

The detuning choice ensures that phonons cannot hop from one resonator to the other via the auxiliary mode. The final result of this treatment is a new, enhanced damping rate  $\Gamma_{\text{eff}}$ . However, the noise strength in the Langevin equations is unchanged. We can write

$$\tilde{b} = \dots + \sqrt{\Gamma_m} b_{\text{in}} = \dots + \sqrt{\Gamma_{\text{eff}}} \tilde{b}_{\text{in}}, \quad (\text{S41})$$

where the new effective noise has correlators  $\langle \tilde{b}_{\text{in}}(t) \tilde{b}_{\text{in}}^\dagger(t') \rangle = n_{\text{thermal}} \delta(t - t') \times (\Gamma_m / \Gamma_{\text{eff}})$ . This way we obtain two new effective parameters  $\Gamma_{\text{eff}}$  and  $n_{\text{eff}} = n_{\text{thermal}} \Gamma_m / \Gamma_{\text{eff}}$ , with the remainder of the Langevin equations unchanged.

## CONNECTION TO METELMANN AND CLERK RECIPE FOR NONRECIPROCITY [S16]

In this section we relate the calculations in the main text to the method for constructing nonreciprocal interactions presented in [S16]. Clearly, both conditions in Eq. (S7) can only be fulfilled for complex susceptibilities, underscoring the importance of dissipation. In order to distinguish coherent and dissipative parts of the coupling, we compare Eq. (3) with the equations of motion for a nondegenerate parametric amplifier with interaction Hamiltonian

$$H_{\text{int}} = \lambda a_1^\dagger a_2^\dagger + \text{H.c.}, \quad (\text{S42})$$

namely

$$\left( \frac{\kappa_1}{2} + \partial_t \right) \langle \vec{A}_1 \rangle = i \begin{pmatrix} 0 & -\lambda \\ \lambda^* & 0 \end{pmatrix} \langle \vec{A}_2 \rangle, \quad \left( \frac{\kappa_2}{2} + \partial_t \right) \langle \vec{A}_2 \rangle = i \begin{pmatrix} 0 & -\lambda \\ \lambda^* & 0 \end{pmatrix} \langle \vec{A}_1 \rangle, \quad (\text{S43})$$

where  $\vec{A}_i \equiv (a_i, a_i^\dagger)^T$ . The phase of  $\lambda$  is arbitrary, as it is determined by the origin of time when going into the rotating frame. Equation (S43) suggests that coherent and dissipative interaction mediated by the mechanical resonators are the sum and difference of  $iT_{12}$  and  $iT_{21}$ . Thus, the coherent part is

$$\lambda = \sum_i \text{Re}[\chi_{m,i}(0)] G_{i1} J_{i2} = \sum_i \frac{2\Gamma_{m,i} G_{i1} J_{i2}}{\Gamma_{m,i}^2 + 4\delta_i^2}, \quad (\text{S44})$$

whereas the dissipative part of the interaction is

$$i\sigma = \sum_i i \operatorname{Im}[\chi_{m,i}(0)] G_{i1} J_{i2} = i \sum_i \frac{4\delta_i G_{i1} J_{i2}}{\Gamma_{m,i}^2 + 4\delta_i^2}. \quad (\text{S45})$$

nonreciprocity is achieved if  $\lambda + i\sigma = 0$  but  $\lambda, \sigma \neq 0$ , such that  $\lambda - i\sigma \neq 0$ , a condition that the driving strengths Eq. (5) in the main text fulfill. For the DPPA, with Eq. (5), and  $C_1 = 1$  for simplicity, the equations of motion are

$$(\kappa_1 + \partial_t) \langle \vec{A}_1 \rangle = i \begin{pmatrix} 0 & -\lambda - i\sigma \\ \lambda^* - i\sigma^* & 0 \end{pmatrix} \langle \vec{A}_2 \rangle = 0, \quad (\text{S46a})$$

$$\left[ \frac{\kappa_2}{2} (1 - C_2) + \partial_t \right] \langle \vec{A}_2 \rangle = i \begin{pmatrix} 0 & -\lambda + i\sigma \\ \lambda^* + i\sigma^* & 0 \end{pmatrix} \langle \vec{A}_1 \rangle = 2i \begin{pmatrix} 0 & \lambda \\ -\lambda^* & 0 \end{pmatrix} \langle \vec{A}_1 \rangle, \quad (\text{S46b})$$

with

$$\lambda = i\mathbf{T}_{12}(0)/2. \quad (\text{S47})$$

Now that we have discerned which part of the interaction is dissipative and which is coherent, we can map onto a quantum master equation. Following [S16], the way to make a coherent interaction  $H = J a_1^\dagger a_2^\dagger + \text{H.c.}$  directional is by introducing a dissipative term in the QME of the form  $\Gamma \mathcal{L}[z]\rho$ , with

$$z = \sqrt{2}(\cos \theta a_1 + e^{i\varphi} \sin \theta a_2^\dagger). \quad (\text{S48})$$

Directionality is obtained for the appropriate choice of  $\theta$  and  $\varphi$ . Indeed, we have

$$\langle \dot{a}_1 \rangle = -(\kappa_1/2 + \Gamma \cos^2 \theta) \langle a_1 \rangle + (iJ - \Gamma \sin \theta \cos \theta e^{i\varphi}) \langle a_2^\dagger \rangle, \quad (\text{S49a})$$

$$\langle \dot{a}_2^\dagger \rangle = -(\kappa_2/2 - \Gamma \sin^2 \theta) \langle a_2^\dagger \rangle - (iJ^* - \Gamma \sin \theta \cos \theta e^{-i\varphi}) \langle a_1 \rangle. \quad (\text{S49b})$$

Setting  $\Gamma$  and  $\theta$  such that  $\Gamma \sin \theta \cos \theta e^{i\varphi} = iJ$ ,

$$\left( \frac{\kappa_1}{2} + |J \cot \theta| + \partial_t \right) \langle a_1 \rangle = 0, \quad (\text{S50a})$$

$$\left( \frac{\kappa_2}{2} - |J \tan \theta| + \partial_t \right) \langle a_2^\dagger \rangle = -2iJ^* \langle a_1 \rangle. \quad (\text{S50b})$$

With  $J = \lambda$ , the RHS of Eq. (S50) matches Eq. (S46).

In order to appropriately map the Langevin equations onto a master equation, we have to take into account that there are *two* coherent interactions and *two* baths. Therefore, we have to repeat this procedure twice, making the two parts of the coherent interaction

$$i\lambda_1 = \operatorname{Re}[\chi_{m,1}(0)] G_{11} J_{12} = \frac{\sqrt{\kappa_1 \kappa_2 C_2}}{4} e^{i\Phi/2}, \quad (\text{S51a})$$

$$i\lambda_2 = \operatorname{Re}[\chi_{m,2}(0)] G_{21} J_{22} = \frac{\sqrt{\kappa_1 \kappa_2 C_2}}{4} e^{-i\Phi/2} \quad (\text{S51b})$$

individually directional. This yields

$$\left( \frac{\kappa_1}{2} + \sum_i |\lambda_i \cot \theta_i| + \partial_t \right) \langle a_1 \rangle = 0, \quad (\text{S52a})$$

$$\left( \frac{\kappa_2}{2} - \sum_i |\lambda_i \tan \theta_i| + \partial_t \right) \langle a_2^\dagger \rangle = -2(i\lambda_1^* + i\lambda_2^*) \langle a_1 \rangle. \quad (\text{S52b})$$

Impedance matching gives  $\tan \theta_i = 4|\lambda_i|/\kappa_i$ , and we recover Eq. (S46).

To illustrate why two baths are necessary, consider again Eq. (S50), which only has one bath. Choosing  $\theta$  such that  $|\cot \theta| = \kappa_1/(2|J|)$  (impedance matching), we do not quite recover Eq. (S46), but instead find

$$\frac{\kappa_2}{2} (1 - C_2/2) \langle a_2^\dagger \rangle = -2i\lambda^* \langle a_1 \rangle. \quad (\text{S53})$$



Whilst this leads to the same interaction (RHS), the self-energies on the LHS differ. Therefore, we need to theoretically include both baths in order to obtain an accurate representation of our system. The reason for the factor of 2 difference lies in the fact that the coherent interactions differ by  $\pi/2$  in phase, such that  $|\lambda| = (|\lambda_1| + |\lambda_2|)/\sqrt{2}$  [cf. Eq. (S47)].

- 
- [S1] C. Gardiner and P. Zoller, *Quantum Noise: A Handbook of Markovian and Non-Markovian Quantum Stochastic Methods with Applications to Quantum Optics*, Springer Series in Synergetics (Springer, 2004).
  - [S2] M. Aspelmeyer, T. J. Kippenberg, and F. Marquardt, *Reviews of Modern Physics* **86**, 1391 (2014).
  - [S3] C. W. Gardiner and M. J. Collett, *Physical Review A* **31**, 3761 (1985).
  - [S4] G. A. Peterson, F. Lecocq, K. Cicak, R. W. Simmonds, J. Aumentado, and J. D. Teufel, [arXiv:1703.05269](#).
  - [S5] N. R. Bernier, L. D. Tóth, A. Koottandavida, A. Nunnenkamp, A. K. Feofanov, and T. J. Kippenberg, [arXiv:1612.08223](#).
  - [S6] D. Malz and A. Nunnenkamp, *Physical Review A* **94**, 023803 (2016), [arXiv:1605.04749](#).
  - [S7] D. Malz and A. Nunnenkamp, *Physical Review A* **94**, 053820 (2016), [arXiv:1610.00154](#).
  - [S8] A. Metelmann and A. A. Clerk, *Physical Review X* **5**, 021025 (2015), [arXiv:1502.07274](#).
-